

# A novel packaging method for FBG temperature sensors based on ultrasonic-assisted soldering technology

Xueli Yang <sup>a,b,\*</sup>, Mingyao Liu <sup>a,b</sup>, Han Song <sup>a,b</sup>, Jun Rao <sup>a,b</sup>, Yihang Wu <sup>a,b</sup><sup>7</sup>

<sup>a</sup> School of Mechanical and Electronic Engineering, Wuhan University of Technology, 122 Luoshi Road, Wuhan 430070, China

<sup>b</sup> Hubei Digital Manufacturing Key Laboratory, Wuhan University of Technology, 122 Luoshi Road, Wuhan 430070, China

## ARTICLE INFO

**Keywords:** <sup>5</sup>  
Packaging technology  
FBG temperature sensors  
Invar alloy  
Sn-based soldering material  
Ultrasonic assisted soldering

## ABSTRACT

The packaging technology of fiber Bragg grating (FBG) sensors is the key to determining their operational performance. A method for encapsulating FBG temperature sensors using ultrasonic-assisted soldering technology has been proposed and attempted. This packaging method is based on the successful connection between SiO<sub>2</sub> quartz glass and Invar alloy. Implementing this soldering connection depends on the active components in the solder, which are dispersed into SiO<sub>2</sub> and metal alloys to form more stable substances. The FBG with the removed coating is reliably connected to the metal capillary through ultrasonic soldering. The fragile FBG is adequately protected in the capillary. Sn-based solder with a melting point of 297 °C has been selected. The soldering temperature of 330 °C avoids significant residual stress caused by the difference in the thermal expansion coefficient of the material at the joint. Excellent bonding strength between optical fibers, solder, and capillaries is necessary for encapsulating sensors. Compared to adhesive, solder packaging is no longer affected by the creep of the sealant. The results show that the working range of FBG temperature sensors encapsulated in epoxy resin is -25 °C – 115 °C, while temperature sensors encapsulated by welding can operate stably at -50 °C – 280 °C. Sensors packaged using ultrasonic-assisted soldering technology have the potential to be embedded in metal substrates, creating favorable conditions for the development of intelligent electromechanical components.

## 1. Introduction

Fiber Bragg grating (FBG) temperature sensors are brought into sharp focus in the temperature monitoring field of aerospace electro-mechanical systems due to their unparalleled advantages, such as lightweight, small size, corrosion resistance, and resistance to electromagnetic interference [1,2]. Fragile FBGs require reasonable packaging, a prerequisite for their practical application [3]. The most common packaging forms for FBG temperature sensors include fiber optic metallization and capillary encapsulation. However, both current packaging methods have certain drawbacks in their application. There is a risk of separating the metal and fiber layers of metalized FBG under variable temperature conditions. Capillary temperature sensors that rely on epoxy resin sealing face issues such as inaccurate measurement and narrow measurement range, which are limited by the failure of epoxy resin under high temperature conditions. Exploring better packaging methods is an inevitable path to optimize FBG temperature sensors. Based on fully understanding the mechanism and application of soldering technology, this paper introduces the technology into the field of

sensor packaging for the first time, which will exploit a new route for this field.

In recent years, significant efforts have been made in the soldering technology of dissimilar materials. In the field of sensor packaging, the soldering connection between metal alloys and SiO<sub>2</sub> f/SiO<sub>2</sub> composite materials and between metal alloys and SiO<sub>2</sub> quartz materials has attracted much attention. Ag-Cu-Ti solder exhibits superiority in connecting this heterogeneous material due to its good metallurgical bonding and plasticity with SiO<sub>2</sub>. Wu et al. [4] have achieved solid-state bonding of SiO<sub>2</sub> f/SiO<sub>2</sub> composite materials with Al<sub>2</sub>O<sub>3</sub> ceramics with the help of Ag-Cu-Ti active fillers. However, the Ag-Cu-Ti solder requires a working environment with high temperature and vacuum, significantly limiting its application field. In addition, the significant mismatch in the thermal expansion coefficient between SiO<sub>2</sub> and metal coupling at high temperatures leads to a significant decrease in joint strength. Three commonly used methods have been announced to reduce residual thermal stress in welded joints: 1 Improving solder wettability by adding active substances [5]. 2. Install a buffer layer with thermal expansion between the substrates to be welded. Such as molybdenum, cobalt, etc.

\* Corresponding author at: School of Mechanical and Electronic Engineering, Wuhan University of Technology, 122 Luoshi Road, Wuhan 430070, China.  
E-mail address: [yxueli@whut.edu.cn](mailto:yxueli@whut.edu.cn) (X. Yang).

[6]. 3. Low-temperature solder replaces high-temperature solder and introduces ultrasonic-assisted soldering. Ultrasonic-assisted soldering technology can achieve welding in low-temperature and nonvacuum environments, and this technology has been widely applied to the connection of different materials. The energy of ultrasonic vibration can effectively remove the oxide film on the material surface, improve its wettability, and refine its grain size. Zhou et al. [7] deposited a Cu film on the surface of alumina ( $\text{Al}_2\text{O}_3$ ) ceramics using magnetron sputtering, and then connected the ceramics to AA2024 using ultrasonic assisted welding. Wu et al. [8] have achieved metal welded silicon glass with Sn-2Ti solder as filler at a low temperature of 250 °C. References [9,10] have used Sn-9Zn-2Al solder and Sn-Bi solder separately to perfectly weld quartz glass and 2024 aluminum alloy together under ultrasonic assistance, then analyzed the welding mechanism and joint strength. Li et al. [11] have applied Zn5Al solder to connect 2024Al and  $\text{Al}_2\text{O}_3$  ceramics with the assistance of ultrasonic brazing process. And cool the welded joints in the furnace to obtain smaller residual stresses in the joints. In summary, ultrasonic-assisted soldering technology has achieved outstanding results in welding dissimilar materials. Considering that the fiber optic material is  $\text{SiO}_2$  quartz, the paper introduces this technology into the packaging field of quartz fiber optic sensors for the first time.

In fiber optic sensor packaging, epoxy resin bonding and metallization of optical fiber are the most common packaging methods. Yang et al. [12,13] have developed two types of capillary temperature sensors: FBGs encapsulated in high thermal expansion copper capillary and encapsulated in Invar capillary with an ultra-low thermal expansion coefficient. Copper capillary packaging brings high sensitivity, while Invar alloy packaging is more stable. However, both sensors are limited in their measurement range by the creep characteristics of epoxy resin. The so-called creep is the continuous deformation process of a material under external forces, when it is exposed to high temperatures for a long time. Epoxy resin typically begins to creep at around 100 °C. Therefore, the adhesive prone to failure is not the preferred choice for encapsulating sensors. In this situation, the metallization process of FBG is gradually becoming popular. The bare fiber surface is coated with a metal layer to protect the fiber itself [14]. Xiao et al. [15] have painted a layer of Ti (approximately 1 μm thick) on the surface of FBG by magnetron sputtering to improve the adhesion and bonding between the metal layer and fibers. Then, they have applied a layer of Ni to increase the thickness of the metal layer. Magnetron sputtering is a physical vapor deposition technique that deposits thin films by controlling the magnetic field. This technology has developed into one of the most important technologies in industrial coatings. The first step in metallization of optical fibers requires the use of this process to prepare conductive thin films. The outer layer of the thin film is coated with a metal layer through electroplating process to protect the optical fiber. However, the uniformity and thickness of the metal layer are difficult to control and accurately control. The adhesion between the coating and bare fibers still needs to be improved. In high-temperature environments, due to significant differences in the thermal expansion coefficient of materials, there may also be a separation between metal coatings and optical fibers. Therefore, the above two packaging methods are on the brink of elimination. It is necessary to study new packaging technologies and processes for fiber optic sensors, which is the key to the transition of fiber optic sensors from experimental to practical applications. Ultrasonic-assisted soldering technology is gradually emerging, but it is limited to the level of mechanism research and has yet to rise to practical applications. The difference in thermal expansion coefficient between optical fibers and metal alloys is the main reason for the low strength of welded joints. FBG is packaged and protected using ultra-low thermal expansion coefficient Invar steel. Sn-based solder is excellent for reducing residual thermal stress in welded joints due to its low melting point. The welding feasibility of Invar steel and optical fiber materials is the basis for achieving the welding packaging of sensors. Therefore, this article starts with the soldering process of quartz glass sheets and Invar

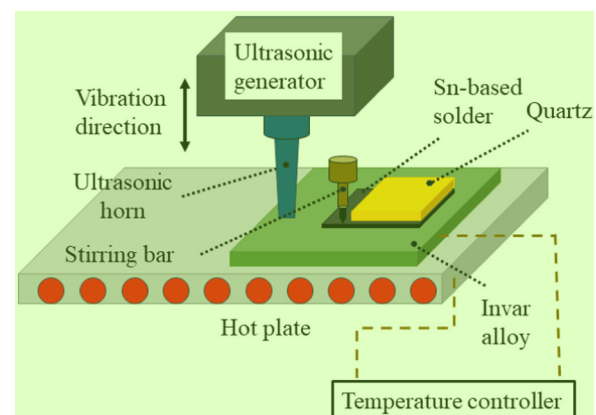


Fig. 1. Schematic diagram of soldering process. 1

alloy sheets and gradually introduces this technology into the fiber optic sensor packaging field. 5

The focus of this article's discussion is the impact of improving 1 packaging methods on increasing the temperature measurement range. Taking the achievable soldering of quartz materials and metal alloys as an opportunity to explore new packaging methods suitable for FBG temperature sensors. The sensor includes quartz fiber and capillary made of Invar alloy. The specific content of this article is as follows: Firstly, with the assistance of ultrasonic technology, a Sn-based solder is used to weld quartz and alloy sheets. Observation and testing have been conducted on the welding strength and interface characteristics to verify the reliability of welding. Subsequently, ultrasound-assisted soldering technology has been applied to the packaging field of FBG sensors. The two ends of the metal capillary are connected and sealed by soldering and inserting optical fibers. Finally, the performance of sensors with different packaging methods was compared, including bare FBG, epoxy resin sealing, and solder packaging. Here, bare FBG refers to FBG with or without a thin coating removed. The high and low temperature characteristics and temperature measurement range of these sensors have been tested to verify the advantages of welded packaging.

## 2. Soldering mechanism analysis 2

### 2.1. Soldering of invar and quartz materials 1

At present, research on dissimilar materials' soldering is limited to 3 specific and commonly used materials, such as ceramics, glass, and aluminum alloy and Kovar alloy. The welding of Invar alloy and quartz materials has yet to be attempted. Verifying the feasibility of brazing quartz and Invar materials is a prerequisite for achieving practical applications. Therefore, the first step of this paper is to investigate and analyze the connection between quartz and Invar alloy under ultrasonic assisted soldering. The selection of plate-like quartz glass and Invar steel is convenient for testing welding strength and analyzing welding mechanisms. Before welding begins, polish the quartz glass plate and

Table 1  
The characteristics of several materials to be welded. 1

Material	Melting temperature (°C)	Size (mm)	Thermal expansion coefficient ( $10^{-6}/^{\circ}\text{C}$ )	Young's modulus (GPa)	Poisson's ratio
Quartz	1600	10×10×2	0.55	72	0.17
Invar alloy	1450	20×20×2	1.3	144	0.30
Sn-based solder	297	12×12×0.5	-	-	-

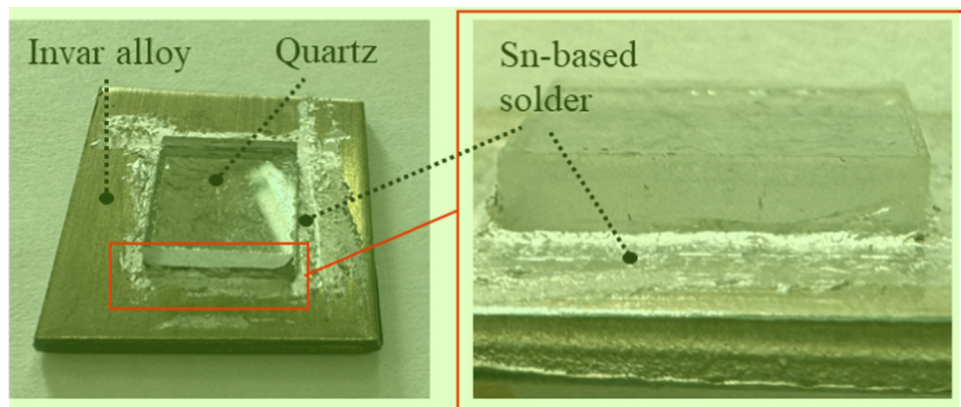


Fig. 2. The specimen after ultrasonic assisted welding. 2

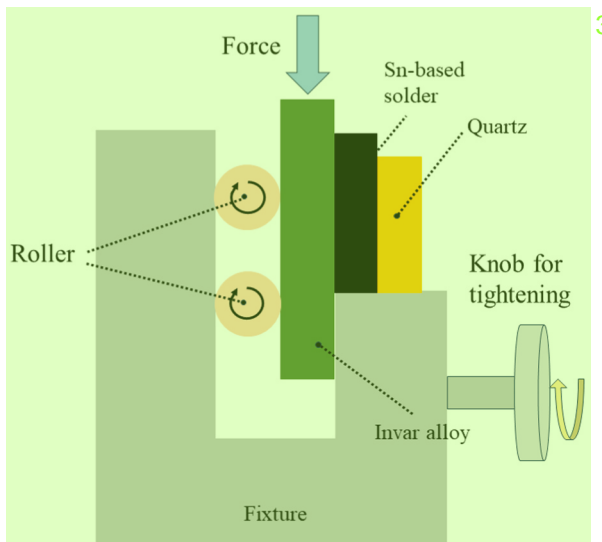


Fig. 3. Schematic diagram of shear force test. In part 4.2, the result of the joint strength is analyzed and discussed in detail.

metal alloy plate and place them together with the soldering material in acetone and alcohol for ultrasonic cleaning for 10 minutes. After cleaning,  $10 \times 10 \times 2\text{mm}$  quartz glass and  $20 \times 20 \times 2\text{ mm}$  Invar alloy are placed on the ultrasonic welding table. Place Sn-based solder (model: CS297) between two objects to be soldered, as shown in Fig. 1. This solder type mainly comprises Sn (30 wt%) and Zn (65 wt%). Zn primarily improves Sn-based alloy's melting point and expands their application range. In addition, elements with solid chemical affinity for oxygen, such as Ti, Si, Al, and rare earth elements, are also included in a 5 wt% proportion. These elements form relatively stable compounds at the interface of the solder, which is an essential reason for achieving reliable connections. Table 1 lists the characteristics of several materials to be welded.

The equipment used in the experiment is an ultrasonic vibration-assisted soldering vibration system with the model USS-9210Mkll. The system mainly consists of four parts: an ultrasonic generator, a heating table, a pressurization device, and a support structure. The heating temperature of the system can reach  $480^\circ\text{C}$ . The temperature control accuracy is  $1^\circ\text{C}$ . The frequency of the ultrasonic drive power supply is 60 KHz.  $3\text{--}10\text{ }\mu\text{m}$  is the output range of amplitude. After multiple attempts, the parameters selected for this experiment are frequency 60 KHz, heating temperature  $330^\circ\text{C}$ , and ultrasonic power 15 W. The welding schematic diagram of silica glass and Invar alloy is shown in Fig. 2. The plate-like quartz glass and Invar alloy are tightly connected

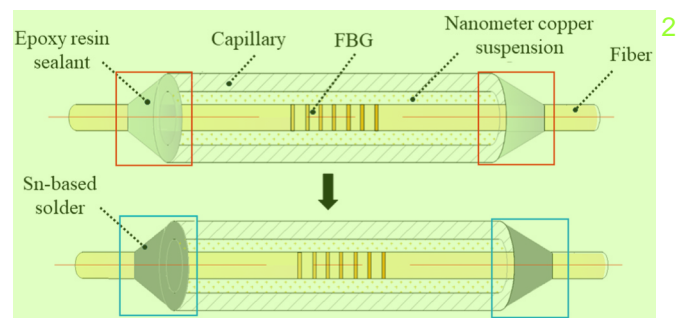


Fig. 4. Structural design of the FBG temperature sensor. 3

by Sn-based solder, forming a whole. 7

## 2.2. Soldering interface microscopic analysis 3

In order to evaluate the welding effect and analyze the welding mechanism, the Leica EM TXP precision grinding integrated machine was used to cut the specimens. Polish the cutting surface with sandpaper of 10 microns and 2 microns in sequence. The field emission scanning electron microscope and X-Max 50 X-ray energy spectrometer were employed to observe the microstructure of the brazed joint interface. The electron microscope model is Zeiss Ultra Plus. The magnification of the electron microscope is 12–1000000X.

In part 4.1, the result of the microstructure of the brazing interface is analyzed and discussed in detail.

## 2.3. Shear force test 2

The shear strength is a key indicator for measuring whether the welded quartz glass and Invar alloy specimens can be put into application. The tensile shear test is an evaluation test of the mechanical properties of welded joints. On the Instron 5967 electronic universal material testing machine, a specially designed shear fixture is used to test the shear strength of welded joints at a testing speed of  $0.027\text{ mm/s}$ , as shown in Fig. 3. The load range of this testing machine is 0–30 KN.

## 3. Sensor structure and packaging process 4

### 3.1. Sensor structure proposal 1

Lightweight and small-sized FBG sensors have been developed for temperature monitoring of compact aerospace electromechanical systems. The sensor comprises a capillary tube, nanometer copper suspension, and a fiber optic grating, as shown in Fig. 4. FBG is protected by

**Table 2**  
FBG temperature sensor related parameters.

Definition	Value
Metal capillary materials in the temperature sensor	Invar alloy ( 4J36 )
Fiber materials in the temperature sensor	Quartz ( $\text{SiO}_2$ )
The diameter of the fiber	0.125 mm
The grating length of the FBG	3 mm
The FBG center wavelength	$1547 \pm 1 \text{ nm}$
The inner diameter of the Invar capillary	0.2 mm
The outer diameter of the Invar capillary	0.4 mm
The length of the temperature sensor	20 mm

capillaries to prevent external damage. The filling of nanometer copper suspension has two essential functions: (1) to avoid inaccurate measurement results caused by FBG shaking in the capillary; (2) the nanometer copper suspension significantly improves the response speed of the sensor. The anti-vibration and fast response performance of this FBG temperature sensor has been fully validated by our previous work [12, 13]. However, the packaging of this FBG temperature sensor relies on epoxy resin adhesive. And the epoxy resin exhibits creep characteristics under temperature changes, limiting the sensor's precise temperature sensing range. Soldering technology has been introduced in sensor packaging to improve sensor performance. Ultrasonic welding replaces epoxy resin adhesive to reduce measurement errors of sensors under variable temperature conditions. In this sensor, the optical fiber and capillary materials are quartz and Invar alloy, respectively. The structural parameters of the sensor are shown in Table 2. Based on previous research and experiments, the sensor structure has good vibration resistance and fast response ability. The focus of this article's discussion is the impact of improving packaging methods on increasing the temperature measurement range.

FBG is an optical passive filter that reflects specific wavelengths of light waves. When a certain width of spectrum passes through FBG, the light waves that meet the Bragg condition are reflected, while the remaining light waves continue to pass through the grating. The Bragg condition for FBG reflection wavelength is:

$$\lambda_B = 2n_{\text{eff}}\Lambda \quad (3)$$

where,  $\lambda_B$  (nm) is the wavelength of the reflected light wave, which is the center wavelength of the FBG.  $n_{\text{eff}}$  is the effective refractive index of fiber core,  $\Lambda$  (nm) is the grating period.

The changes in strain and temperature can cause the center wavelength shift of FBG, as given by (2). The temperature sensitivity of FBG is determined by the thermal expansion and thermal optical effect of optical fibers.

$$\Delta\lambda_B/\lambda_B = (1 - P_e)\epsilon + (\alpha + \xi)\Delta T \quad (2)$$

where,  $P_e$  is the photo-elastic coefficient of the optical fiber,  $P_e = 0.22$ . $\epsilon$  is the strain acting on the FBG.  $\alpha$  ( $^{\circ}\text{C}$ ) and  $\xi$  ( $^{\circ}\text{C}$ ) are the thermal expansion coefficient and thermal optical coefficient of the fiber material, respectively,  $\alpha = 0.55 \times 10^{-6}/^{\circ}\text{C}$ ,  $\xi = 6.67 \times 10^{-6}/^{\circ}\text{C}$ .  $\Delta T$  ( $^{\circ}\text{C}$ ) is the temperature change.

In order to improve the reliability and stability of sensors, ultra-low thermal expansion coefficient Invar steel material is selected to package FBG. Fiber optic and Invar alloy exhibit slight thermal expansion differences under temperature changes, thereby reducing the risk of separation between the two. FBG works in capillaries made of Invar material to avoid breakage and damage. The relationship between FBG wavelength shift and temperature in this capillary temperature sensor follows (3):

$$\Delta\lambda_B/\lambda_B = [\alpha + \xi + (1 - P_e)(\alpha_I - \alpha)]\Delta T \quad (3)$$

where,  $\alpha_I$  ( $^{\circ}\text{C}$ ) is the thermal expansion coefficient of the Invar material,  $\alpha_I = 1.3 \times 10^{-6}/^{\circ}\text{C}$ .

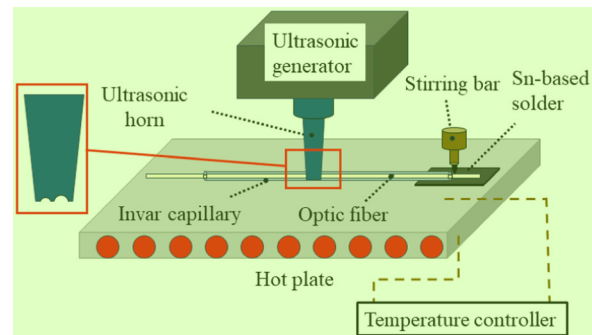


Fig. 5. Schematic diagram of capillary soldering process.

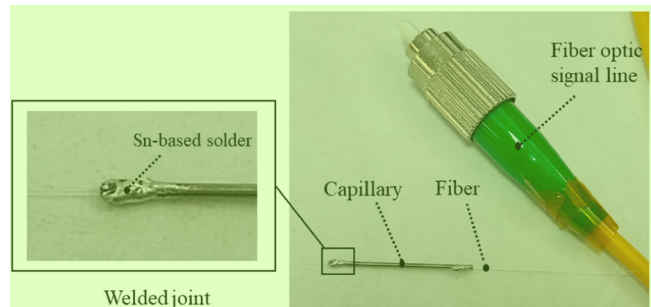


Fig. 6. Physical image of FBG temperature sensor for ultrasonic assisted soldering.

Eq. (3) implies the linearity between FBG wavelength drift and temperature change in temperature sensors. The linear slope is determined by the thermal expansion coefficient of the Invar material, the elastic optical coefficient of the optical fiber, the thermal optical coefficient of the optical fiber, and the thermal expansion coefficient.

### 3.2. FBG temperature sensor's packaging process

The Invar capillary and optical fiber are placed in an ultrasonic cleaning machine and cleaned with alcohol for 10 minutes. Nanometer copper suspension is injected into the capillary tube through a micro syringe with an outer diameter of 0.16 mm. The injection volume of the nanometer copper suspension can be clearly observed through the syringe chamber made of transparent silicon glass. After filling is complete, the capillary action of the capillary tube prevents the suspension from easily leaking. After that, insert the bare fiber into a capillary filled with suspension. The FBG grating region is located at the center of the Invar capillary. Apply a layer of Sn-based solder to both ends of the capillary tube to ensure that the suspension does not leak during the welding process. The excellent effect of completely filling gaps with nano copper suspension was discussed in detail in our previous work [12]. As a note, there is no bending phenomenon of the bare FBG during the operation process. The fragile bare FBG is protected by capillaries to avoid breakage. Subsequently, A suitable tool head is designed for welding tubular sensors. Specifically, the ultrasonic horn in Fig. 1 is replaced by a horn with a curved groove at the bottom, as shown in Fig. 5. The capillary is limited to the groove for fixation and positioning. Sn-based solder connects the capillary and optical fibers under ultrasonic-assisted soldering to achieve sensor encapsulation, as shown in Fig. 6.

As a note, in practical applications, a protective cover has been used to wrap the optical fiber to avoid sharp transitions at the welded joint.

**Table 3**  
Relevant parameters of the temperature control cabinet and interrogator.

Definition	Value
Temperature range of the temperature control cabinet	0–70 °C
The accuracy of the temperature control cabinet	$\pm 0.1 \pm 0.2$ °C
The resolution of the temperature control cabinet	0.1 °C
The range of demodulation wavelength of the interrogator	1530–1570 nm
The resolution of the interrogator	0.1 pm
The sampling frequency of the interrogator	100

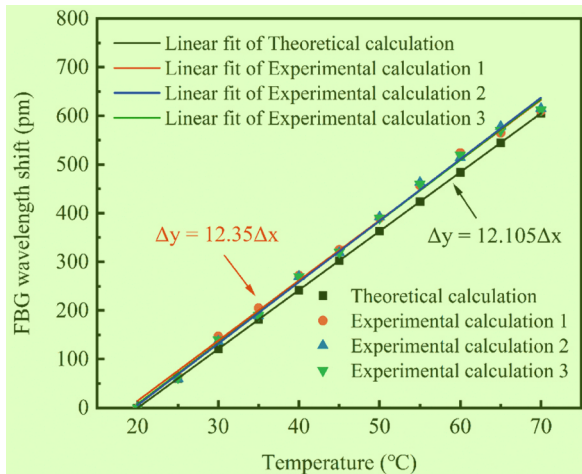


**Fig. 7.** Experimental calibration and theoretical calculation results of FBG temperature sensors.

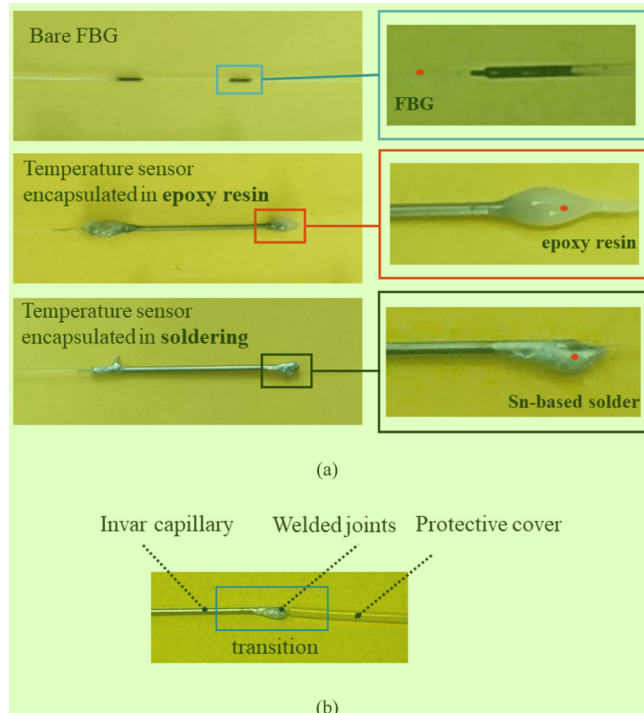


**Fig. 8.** The physical objects of the FBG temperature sensors. (a) FBG temperature sensors with three different packaging methods. (b) Protection scheme for the soldering joint.

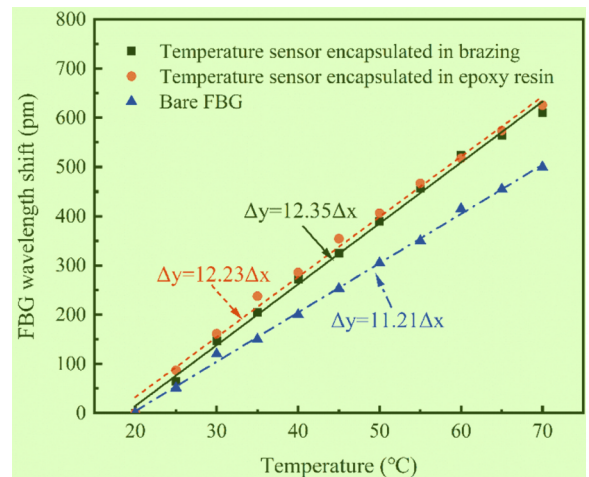


**Fig. 9.** Temperature response performance of three types of sensors.

### 3.3. FBG temperature sensor's calibration

The FBG temperature sensor packaged by ultrasonic-assisted soldering is placed in a temperature control cabinet for calibration experiments. The temperature change step inside the temperature control cabinet is 5 °C. 20 °C and 70 °C are the upper and lower limits in temperature calibration experiments, respectively. The optical sensing interrogator records the shift of the center wavelength of the FBG. The relevant parameters of the temperature control cabinet and interrogator are listed in Table 3. The calibration experiment was repeated three times in the same environment. The calibration results of the temperature sensor are shown in Fig. 7. The experimental calibration results have a consistent linear upward trend with the theoretical calculation results. The slight difference may come from the thermal effect of solder. In the three repeated calibration experiments, the sensor encapsulated by ultrasonic soldering technology has a highly consistent response, which is the key to accurate sensor measurement.

The sensors are packaged using adhesive and welding methods to compare the temperature characteristics of FBG temperature sensors under different packaging methods, as shown in Fig. 8(a). Among them, the adhesive is epoxy resin. The solder used for brazing is a Sn-based solder. The sharp transition at the fiber optic and welding joints poses a fracture risk. In practical applications, wrapping optical fibers with protective covers to avoid sharp transitions at welded joints, as shown in Fig. 8(b).

The packaged temperature sensor and bare FBG have been calibrated. The calibration structure is shown in Fig. 9. The temperature sensitivity of bare FBG is slightly lower. The sensor encapsulated by epoxy resin and that encapsulated by Sn-based solder have consistent temperature sensitivity, determined by the capillary material's thermal expansion coefficient.

## 4. Results and discussion

### 4.1. Interface tissue morphology

Microscopic magnification is performed to analyze the tissue morphology of the soldering interface between quartz glass and Invar steel material. The microstructure of the welding interface is shown in Fig. 10. Showcased a three-layer sandwich structure. The interface between quartz and solder and Invar steel and solder has no gaps and is not a clear boundary but rather a form of mutual penetration. With the assistance of high-frequency ultrasonic vibration, some Sn-based solder substances penetrate the substrate material. Active elements react with other components in a heating environment to form more stable substances. When combined with oxygen, these elements form special

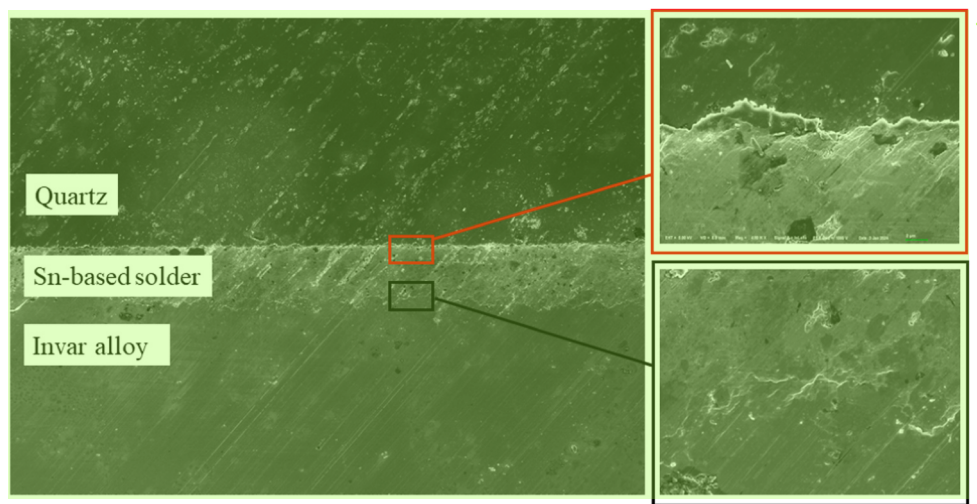


**Fig. 10.** Microscopic morphology of welding interface. 3

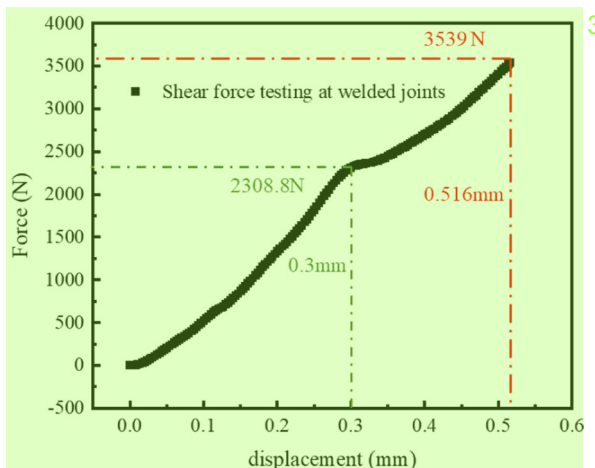


**Fig. 11.** Shear strength test curve of welded section. 2

oxides, thereby establishing chemical bonds between solder, quartz, and Invar alloys. These chemical bonds tightly connect quartz, solder and Invar, so the suitable welding effect is naturally obtained. Furthermore, Sn-based solders penetrate metal alloys more thoroughly, possibly because metal surfaces have more micropores than quartz or because the solder is more likely to react with substances in metal alloys. The microscopic morphology explains the mechanism of ultrasonic-assisted welding. The complete connection between quartz and Invar steel using Sn-based solder is a prerequisite for applying this technology to sensor packaging.

#### 4.2. Shear force properties 1

The electronic universal material testing machine in part 2.3 has been employed to analyze the shear strength of the soldering joint. The welded parts of quartz glass sheets and metal alloys are placed in an electronic universal material testing machine. The force is gradually applied to the cross-section of the Invar alloy. 0.3 mm displacement is the step size. The results show that the welded component can withstand a maximum force of 3539 N, converted into a pressure of 35 MPa, as shown in Fig. 11. There is a singularity at 2308 N, which may be caused by some solder detaching from the substrate.

The performance of this brazed joint is compared and analogized according to the following standards: (1) the shear strength of epoxy resin adhesives is generally around 20 MPa [16]; (2) the standard value

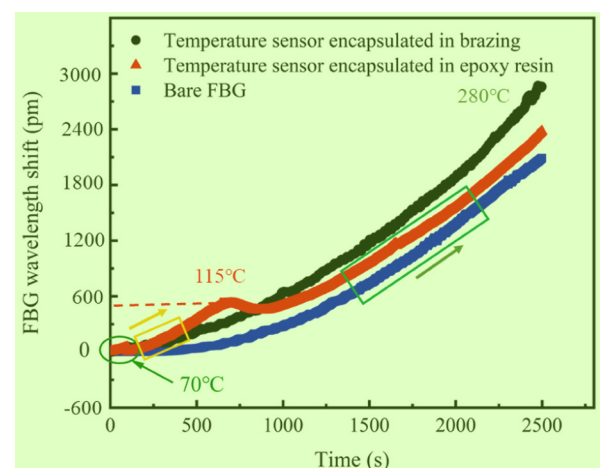


**Fig. 12.** High temperature characteristics of sensors with different packaging technology. 1

for the shear strength of welds made of the same metal material is 45–70 MPa; (3) at present, research has shown that the shear strength of welding samples between various glass materials (including silicate glass, sapphire glass, quartz glass, etc.) and alloys such as copper and titanium, as well as monocrystalline silicon materials, is 14.5–30.2 MPa. The mechanical properties of the weld remain unchanged after 100 cycles of high and low temperatures ranging from  $-55^{\circ}\text{C}$  to  $120^{\circ}\text{C}$ . All performance meets the relevant standard requirements. The shear strength of the sample braze with ultrasonic assistance in this article reaches 35 MPa. Through the above analysis, it can be inferred that the strength can meet the requirements of mechanical performance. The excellent shear strength of the specimen is the foundation and prerequisite for applying this brazing technology in the field of FBG sensor packaging. The excellent shear strength of the specimen is the foundation and prerequisite for applying this brazing technology in the field of FBG sensor packaging.

#### 4.3. High and low temperature testing of sensors 2

A reliable and sturdy interface is formed between quartz and Invar materials through ultrasonic assisted soldering process. Supported by this result, the capillary temperature sensor is packaged using the same principle and operating process. The testing and comparison results of temperature sensors with different packaging at high and low

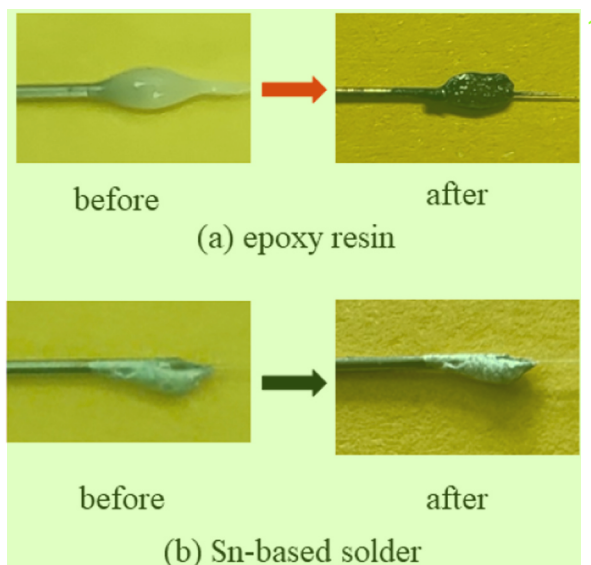


**Fig. 13.** Appearance changes at the sensor packaging before and after high temperature testing.

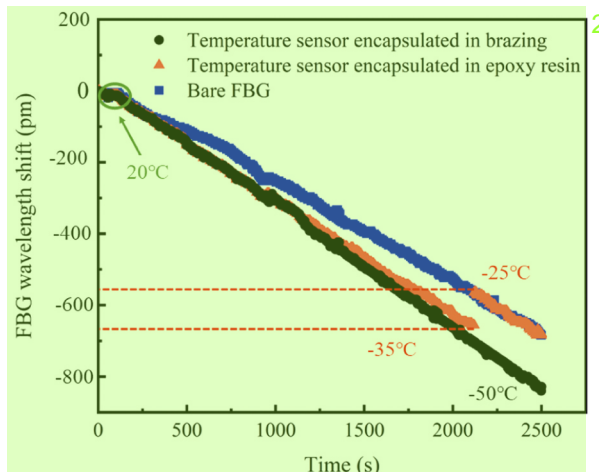


**Fig. 14.** Low temperature characteristics of sensors with different packaging methods.

temperatures are analyzed and discussed.

Three sensors have been placed simultaneously in high-temperature and low-temperature boxes to verify the effect of packaging on the measurement range. Fig. 12 shows the response capability of three sensors to high temperatures. Ultrasonic-assisted soldering sensors have good continuity from 70 °C to 280 °C. Temperature sensors encapsulated in epoxy resin exhibit poor high-temperature resistance. Singularities appear around 115 °C, resulting from the high-temperature failure of epoxy resin. There are two reasons for the high-temperature failure of epoxy resin: (1) the oxidation of hydroxyl and methyl groups in epoxy resin materials leads to changes in their chemical properties; (2) epoxy resin undergoes thermal cracking at high temperatures. The failed epoxy resin exhibits a black appearance, while the formation of the Sn-based solder remains unchanged before and after high-temperature testing, as shown in Fig. 13. Sensors packaged by ultrasonic-assisted soldering exhibit excellent high-temperature characteristics. The sensor still operates below 280 °C, significantly improving its measurement range.

The low-temperature test of the sensor starts at 20 °C and ends at -50 °C, as shown in Fig. 14. The sensor encapsulated in epoxy resin began to exhibit anomalies around -25 °C, with data appearing

discontinuous. The center wavelength of FBG in sensors encapsulated with epoxy resin from 25 °C to -35 °C rebounds, which is the result of the detachment of epoxy resin from FBG. At low temperatures, epoxy resin loses its viscosity, causing capillary tubes to detach from FBG. Sensors encapsulated in epoxy resin exhibit sensing characteristics consistent with bare FBG after 25 °C. Sn-based solder tightly connects the capillary tube and FBG with ultrasound assistance. The brazed sensor exhibits excellent temperature sensing elements between -50 °C and 20 °C.

## 5. Conclusion

In this paper, Invar alloy and quartz glass materials have been successfully connected through ultrasonic-assisted soldering technology. Solder infiltrates quartz glass and Invar steel sheets under the cavitation effect of ultrasonic waves. The shear strength of the welding surface has reached 35 MPa. Furthermore, a new and reliable packaging method for fiber optic sensors has been developed for the first time. (Note: The material of the optical fiber is the same as that of quartz glass, both of which are SiO<sub>2</sub>.) Sn-based solder firmly connects the optical fiber to the Invar capillary with the help of ultrasound. The capillary, a prerequisite for the practical application of sensors, protects the fragile FBG. The selection of Invar material with ultra-low thermal expansion coefficient and Sn-based solder with a low melting point is to avoid significant residual thermal stress at the joint. Compared to adhesive, FBG temperature sensors packaged by soldering have a more comprehensive temperature measurement range. The working range of FBG temperature sensors encapsulated in epoxy resin is -25 °C - 115 °C, while those encapsulated by welding can operate stably at -50 °C - 280 °C. Therefore, sensors packaged by soldering exhibit excellent sensing characteristics in high or low-temperature environments. Ultrasonic-assisted soldering technology has exploited a new route for FBG sensors packaging.

## CRediT authorship contribution statement

**Jun Rao:** Writing – review & editing, Validation. **Han Song:** Writing – review & editing, Supervision, Software. **Yihang Wu:** Investigation. **Mingyao Liu:** Resources, Conceptualization. **Xueli Yang:** Writing – original draft, Validation, Methodology, Investigation, Data curation.

## Declaration of Competing Interest

The authors declare that they have no known competing financial interests or personal relationships that could have appeared to influence the work reported in this paper.

## Data availability

No data was used for the research described in the article.

## References

- [1] Z.H. Liang, D.B. Liu, X. Wang, J. Zhang, et al., FBG-based strain monitoring and temperature compensation for composite tank, *Aerosp. Sci. Technol.* 127 (2022) 107724.
- [2] X.J. Wang, Y.M. Jiang, S.Y. Xu, H. Liu, et al., Fiber Bragg grating-based smart garment for monitoring human body temperature, *Sensors* 22 (2022) 2–14.
- [3] Y. Kuang, Y.X. Guo, L. Xiong, W.L. Liu, Packaging and temperature compensation of fiber Bragg grating for strain sensing: a survey, *Photon. Sens.* 8 (2018) 320–331.
- [4] S.B. Wu, H.P. Xiong, B. Chen, Y.Y. Cheng, Joining of SiO<sub>2f</sub>/SiO<sub>2</sub> composite to Al<sub>2</sub>O<sub>3</sub> ceramic using Ag-Cu-Ti brazing filler metal, *Weld. World* 61 (2017) 181–186.
- [5] L.X. Zhang, Z. Sun, Q. Chang, J.M. Shi, et al., Brazing SiO<sub>2f</sub>/SiO<sub>2</sub> composite to Invar alloy using a novel TiO<sub>2</sub> particle-modified composite braze filler, *Ceram. Int.* 45 (2019) 1698–1709.
- [6] W.W. Li, B. Chen, H.P. Xiong, W.J. Zou, et al., Joining of Cf/SiC composite to GH783 superalloy with NiPdPtAu-Cr filler alloy and a Mo interlayer, *J. Mater. Sci. Technol.* 35 (2019) 2099–2106.

- [7] Z.W. Zhou, H.J. Li, C. Chen, Microstructural transformation and mechanical properties of Cu-sputtered alumina ceramic/Zn5Al/AA2024 ultrasonic soldering joints, *Intermetallics* 165 (2024) 108153.
- [8] X.W. Wu, Z.L. Li, X.G. Song, H.J. Dong, X.Y. Yang, et al., Bonding mechanism of ultrasonically soldered silica glasses using tin-titanium solder filler, *Mater. Lett.* 310 (2022) 131490.
- [9] R.X. Yi, C. Chen, H.J. Li, Y.B. Ma, Ultrasonic soldering silica glass and 2024 alloy in low temperature, *Sci. Technol. Weld. Join.* 27 (2022) 455–462.
- [10] X.L. Gao, C. Chen, High-strength joining of silica glass and 2024 aluminum alloy by ultrasonic-assisted soldering with Sn-Bi low temperature solder, *J. Manuf. Process.* 101 (2023) 1482–1496.
- [11] H.J. Li, Y.X. Li, C. Chen, Microstructure and formation mechanism of Al<sub>2</sub>O<sub>3</sub>/Zn5Al/2024Al joint by ultrasonic assisted soldering process, *J. Manuf. Process.* 83 (2022) 313–324.
- [12] X.L. Yang, M.Y. Liu, H. Song, Y.H. Wu, et al., Nano-copper suspension filling based fabrication and application of FBG temperature sensor with fast response function, *Int. J. Heat. Mass Transf.* 209 (2023) 124085.
- [13] X.L. Yang, M.Y. Liu, H. Song, S.Q. Zhu, et al., Vibration resistance FBG temperature sensor fabrication and its application in the motor for hydraulic pump, *Measurement* 205 (2022) 112141.
- [14] C.Y. Hong, Y.F. Zhang, M.X. Zhang, L.M.G. Leung, et al., Application of FBG sensors for geotechnical health monitoring, a review of sensor design, implementation methods and packaging techniques, *Sens. Actuators A Phys.* 244 (2016) 184–197.
- [15] X.C. Li, F. Prinz, J. Seim, Thermal behavior of a metal embedded fiber Bragg grating sensor, *Smart Mater. Struct.* 10 (2001) 575–579.
- [16] M. Zhao, L.Z. Liu, B. Zhang, M.M. Sun, X.G. Zhang, et al., Epoxy composites with functionalized molybdenum disulfide nanoplatelet additives, *RSC Adv.* (61) (2018) 35170–35178.



**Xueli Yang** was born in Anhui, China, in 1996. She received the Bachelor's degree in Mechanical Engineering from Anhui Polytechnic University, Wuhu, China, in 2019. She is currently working for her doctorate in Mechanical and Electrical Engineering, Wuhan University of Technology, Wuhan, China. Her current research interests include fiber-optical sensors, measurement technology and system, heat and mass transfer, and electromechanical equipment monitoring.

4



**Mingyao Liu** received the M.A. degree from Chongqing University, Chongqing, China, in 1989, and the Ph.D. degree from the Shenyang Institute of Automation, Chinese Academy of Sciences, Shenyang, China, in 2002. In 1994, he was a Visiting Scholar at Tsinghua University, Beijing, China. From 2002–2005, he was a Post-Doctoral Fellow with the Mechanical and Electrical Engineering, Wuhan University of Technology, Wuhan, China. He is currently a Full Professor with Wuhan University of Technology, Wuhan, China. He has presided over five national key projects and has published more than 50 academic papers. His current research interests include fiber optic sensing, equipment condition monitoring, oil extraction equipment, robotics, and mechatronics.



**Han Song** received his B.S. degree in 2010, the M.S. degree in 2012 and the Ph.D. in 2016 from the School of Mechanical Science and Engineering, Huazhong University of Science and Technology, Wuhan, China. He is currently an Associate Professor in the School of Mechanical and Electronic Engineering, Wuhan University of Technology, Wuhan, China. His research interests include optical fiber sensors and micro/nano materials for hydrogen gas detection, FBG sensors for strain, temperature, vibration and pressure measuring.

3



**Rao Jun** was born in Hubei, China, in 1997. He received the master's degree from Wuhan University of Technology, Wuhu, China, in 2023. He is currently working toward his Ph.D. in the School of Mechanical and Electrical Engineering at Wuhan University of Technology, Wuhan, China. His current research focuses on the application and performance of carbon fiber reinforced plastics, electromechanical equipment monitoring.



**Yihang Wu** was born in Hubei, China, in 1994. She received the M.S. degree from college of Engineering, China Agricultural University, Beijing, China, in 2018. She is studying for her doctorate and continues to study with Professor Ming-yao Liu in Mechanical and Electrical Engineering, Wuhan University of Technology, Wuhan, China. Her current research interests include fiber-optical sensors, measurement technology and system, and their industrial applications.